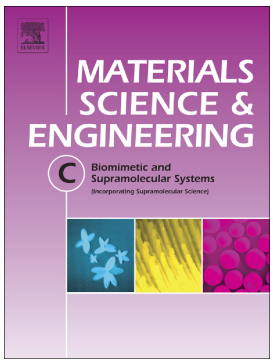

Polyacrylate/polyacrylate-PEG biomaterials obtained by high internal phase emulsions (HIPEs) with tailorable drug release and effective mechanical and biological properties

Marco Corti, Enrica Calleri, Sara Perteghella, Anna Ferrara, Roberto Tamma, Chiara Milanese, Delia Mandracchia, Gloria Brusotti, Maria Luisa Torre, Domenico Ribatti, Ferdinando Auricchio, Gabriella Massolini, Giuseppe Tripodo

PII: S0928-4931(19)31344-X

DOI: https://doi.org/10.1016/j.msec.2019.110060

Reference: MSC 110060

To appear in: *Materials Science & Engineering C*

Received date: 10 April 2019

Revised date: 22 July 2019

Accepted date: 7 August 2019

Please cite this article as: M. Corti, E. Calleri, S. Perteghella, et al., Polyacrylate/ polyacrylate-PEG biomaterials obtained by high internal phase emulsions (HIPEs) with tailorable drug release and effective mechanical and biological properties, *Materials Science & Engineering C* (2019), https://doi.org/10.1016/j.msec.2019.110060

Polyacrylate/Polyacrylate-PEG biomaterials obtained by high internal phase emulsions (HIPEs) with tailorable drug release and effective mechanical and biological properties

Marco Corti [1, †], Enrica Calleri[1, †, *], Sara Perteghella [1], Anna Ferrara [2], Roberto Tamma [3], Chiara Milanese [4], Delia Mandracchia [5], Gloria Brusotti [1], Maria Luisa Torre [1], Domenico Ribatti [3], Ferdinando Auricchio [2], Gabriella Massolini [1], Giuseppe Tripodo [1, *]

[1] Department of Drug Sciences, University of Pavia, Viale Taramelli 12-14, Pavia, 27100, Italy.
[2] Department of Civil Engineering and Architecture, University of Pavia, Via Adolfo Ferrata 3, Pavia, 27100, Italy.
[3] Department of Basic Medical Sciences, Neurosciences, and Sensory Organs, University of Bari Medical School, Piazza Giulio Cesare 11, Bari, 70100, Italy.
[4] C.S.G.I. - Department of Chemistry, Physical-Chemistry Section, University of Pavia, Viale Taramelli 16, Pavia, 27100, Italy.
[5] Department of Pharmacy-Drug Sciences, University of Bari "Aldo Moro", Via Orabona 4, Bari, 70125, Italy.
[†]Marco Corti and Enrica Calleri contributed equally to this work

[*]Corresponding authors, E-mail: giuseppe.tripodo@unipv.it; enrica.calleri@unipv.it

Abstract

The paper focuses on the preparation of polyacrylate based biomaterials designed as patches for dermal/transdermal drug delivery using materials obtained by the high internal phase emulsion (HIPE) technique. In particular, butyl acrylate and glycidyl methacrylate were selected, respectively, as backbone and functional monomer while two different crosslinkers, bifunctional or trifunctional, were used to form the covalent network. The influence of PEG on the main properties of the materials was also investigated. The obtained materials show a characteristic and interconnected internal structure as confirmed by SEM studies. By an industrial point of view, an interesting feature of this system is that it can be shaped as needed, in any form and thickness. The physiochemically characterized materials showed a tailorable curcumin (model of hydrophobic drugs) drug release, effective mechanical properties and cell viability and resulted neither pro nor anti-angiogenic as demonstrated in vivo by the chick embryo choriallantoic membrane (CAM) assay. Based on these results, the obtained polyHIPEs could be proposed as devices for dermal/transdermal drug delivery and/or for the direct application on wounded skin.

Keywords: high internal phase emulsions, biomaterials, acrylates, curcumin, drug delivery

1. Introduction

Polymer-based drug delivery systems have been widely explored in medicine in the last twenty years.[1, 2] Three-dimensional porous scaffolds (3D) represent the first class of biomaterials applied in biotechnological fields such as controlled delivery of drugs in long-term therapies and cell growth supports.[3] 3D porous scaffolds are considered as polymer-based materials with an internal interconnected structure.[4] Biomaterial-based scaffolds may be formulated also as fibers [5] or hydrogels synthetized by the cross-linking of hydrophilic polymeric structures.[4, 6, 7] Lately, even classical drug delivery systems (DDSs) were formulated from new biocompatible building blocks leading to more sustainable systems to provide a controlled release involving different drug delivery technologies.[8]

According to the literature, many different approaches were proposed to achieve biomaterial-based scaffold such as: freeze-drying,[9] salt leaching,[10] gas foaming,[11] supercritical fluid,[12] melt molding,[13] electro spinning[13] and thermally induced phase separation.[13]

The High Internal Phase Emulsion (HIPE) technique is emerging as a valid tool, also in the pharmaceutical field, by emulsion-templating of polymeric materials. HIPEs are typically water in oil (W/O) emulsions with an internal to external phase volume ratio higher than 0.70 (meaning more than 70 % v/v of internal phase). By the polymerization of the external phase of a HIPE (or by using a pre-synthesized polymer) and the subsequent removal of the internal phase, a porous polymeric material with a high degree of internal interconnections, defined polyHIPE (polymerized high internal phase emulsion), could be achieved.[14, 15] In theory, all the known polymerization techniques such as, e.g., free radical polymerization,[16] step growth,[17] atom transfer radical polymerization[18] or ROMP,[19] could be used to polymerize the external phase, thus enormously increasing the versatility of the HIPE technique. After polymerization of the external phase, the internal phase will leave place to cavities (typically named “voids”) that are reciprocally interconnected through secondary pores or channels (throats) leading to an open-porous/highly-interconnected structure. Both voids and throats are considered as macropores.[16] These

interconnecting pores are generated by the rupture (contraction) of the polymeric film during the polymerization step.[20] According to the literature, many synthetic conditions can influence the polyHIPEs internal structure such as the kind and concentration of surfactants,[21] the volume of internal phase[16] and the effect of other stabilizers (particles in the "pickering" type HIPE[22]).

Due to their chemical and process versatility, polyHIPEs systems are increasingly applied as templates for porous materials with tailorable properties and structures.[23] Important applications of polyHIPEs are in: cosmetic and food industry,[24] chromatography,[25] 3D printing,[26] catalysis,[27] enzyme immobilization,[28] electrode material of supercapacitors[29] and absorption of warfare chemical agents.[30] PolyHIPEs may also be proposed for biomedical application (i.e. tissue engineering or drug delivery system) by the synthesis of biodegradable and biocompatible emulsion-templated materials. In literature, different strategies have been shown to achieve biomaterials-based polyHIPEs such as hydrogel-based polyHIPEs[31] or by using biocompatible building blocks.[32] For example, in 2009 Lumelsky and co-workers produced a polyHIPE suitable for tissue engineering using t-butil acryate as principal backbone monomer.[33] Other works suggest the use of polyacrylate (biocompatible materials widely used for biomedical application[34]) for the development of polyHIPEs suitable for biomedical purposes.[28, 35]

While the application of polyHIPE-based biocompatible scaffolds in tissue engineering is reported in literature[36, 37], at the best of our knowledge, the use of polyHIPE-based materials for the preparation of drug delivery systems is not described.

This work is specifically aimed at establishing the main behaviors of acrylate-based polyHIPEs for drug delivery applications since a so conceived drug delivery system (DDS) would benefit from the possibility to co-deliver hydrophobic drugs and biotechnological molecules through direct conjugation to the functional moieties of the designed polyHIPEs. These behaviors were evaluated on different materials obtained by using butyl acrylate as the monomer forming the polymeric backbone, glycidyl methacrylate as a functional monomer bearing epoxy groups for post-production derivatization, e.g., with hydrophilic biomolecules and two different crosslinker, one tri-functional

and one bifunctional to evaluate their effect on the mechanical behaviors of the final materials. Furthermore, a PEG mono-methacrylate was introduced in the formulation with the aim to modify the hydrophilic behaviors of the material surfaces (internal and external) and to evaluate its influence on the internal structure of the corresponding polyHIPEs or on the drug release properties of the material.

2. Experimental Section

2.1 Materials

Trimethylolpropane triacrylate (TMPT), Butyl acrylate (BA), Potassium persulfate (KPS), Glycidyl methacrylate (GMA), PEG methacrylate (PEGMA, Mn 360 as from vendor specifics), 1,6-Hexandiol dimethacrylate (HDMA), N,N,N',N'-Tetramethylethylendiamine (TEMED), Monobasic potassium phosphate (KH_2PO_4), Dibasic sodium phosphate (Na_2HPO_4) NaCl, KCl, tetrahydrofuran (THF), absolute ethanol (EtOH), methanol (MeOH), acetonitrile (CH_3CN), acetic acid, 3-(4,5-dimethylthiazol-2-yl)-2,5-diphenyl-tetrazolium bromide (MTT), dimethyl sulfoxide, 30 mL Syringe PP/PE without needle luer lock tip and female luer coupler in polypropylene were from Sigma-Aldrich (Milan, Italy). Synperonic PE/L 121® was kindly provided by Croda Italiana Spa. The water used in this study was double deionized water (DDW), obtained by a Milli-q system from Millipore. All reagents used for cell culture were purchased from Euroclone (Milan, Italy).

2.2 Apparatus

2.2.1 Scanning electron microscopy

SEM images were acquired on gold sputtered samples using a Zeiss EVO MA10 instrument (Carl Zeiss, Oberkochen, Germany).

2.2.2 High performance liquid chromatography

Chromatographic analysis were carried out using an Agilent technology HP-1100 HPLC instrument (Palo Alto, CA-USA) equipped with a quaternary pump, a Rheodyne injection valve (20 μl), a degasser, an UV-Vis detector set at 420nm, a thermostat oven (25 ± 0.5°C) and an Agilent Technologies LiChrospher 100 RP-18 5μm (250 × 4 mm ID) column. The chromatographic conditions applied were: isocratic elution of a mobile phase composed by water:acetonitrile (55/45 v/v) containing 5 % acetic acid at 0.8 ml/min as flow rate. To quantify the unknown CUR amount in the sample, a calibration curve ($y = 52606\ x - 374.78$; $R^2 = 0.9992$) was performed by the injection of standard solutions of CUR in THF at known concentration (calibration range 0,002 g/L – 0,2

g/L). All the injections were conducted in triplicate for six CUR concentration within the indicated range.

2.2.3 Mechanical characterization

Tensile tests were performed by using a MTS Insight Testing System device (MTS System Corporation) equipped with a 250 N load-cell, two pneumatic grips, and a video extensometer (model ME-46 Messphysik, Fürstenfeld, Austria). For compression tests, the MTS system was equipped with a 10 kN load-cell and two compression plates, whereas the video extensometer was not used due to the specimen shortness.

2.2.4 3D Printing

The dog-bone and cylindrical molds were printed in-home with the Objet260 Connex3 3D printer (Stratasys).

2.3 Methods

2.3.1 PolyHIPE synthesis

The monolithic materials were prepared by the radical polymerization of W/O emulsions characterized by a large volume of internal phase. For the different compositions refer to **Table 1**.

Table 1. Composition parameters for the prepared HIPEs.

	Oil phase			Water phase	
Sample	BA/GMA/Surfactant (ml)	TMPTA (ml)	HDMA (ml)	DDW (ml)	PEGMA (ml)
3.2	4.5/1.8/0.5	1.20	/	31.00	1.00
3.5	4.5/1.8/0.5	1.20	/	31.25	0.75
3.7	4.5/1.8/0.5	/	1.20	32.00	/
3.8	4.5/1.8/0.5	/	1.20	31.25	0.75
3.10	4.5/1.8/0.5	/	1.40	32.00	/
3.11	4.5/1.8/0.5	/	0.80	32.00	/
3.12	4.5/1.8/0.5	/	1.20	31.00	1.00
3.14	4.5/1.8/0.5	/	1.00	31.00	1.00
3.15	4.5/1.8/0.5	/	1.4	30.80	1.2
3.16	4.5/1.8/0.5	/	0.8	31	1

2.3.2 HIPEs Preparation

In this work, HIPEs were prepared following a previously reported procedure[28, 35]. Briefly the oil phase was prepared by mixing in a 2 necks round bottom glass flask butyl acrylate (BA) and glycidyl methacrylate (GMA), backbone and functional lipophilic monomers respectively. Synperonic PE/L 121 was used as polymeric surfactant and an established amount of crosslinker (trimethylpropanetriacrylate [TMPTA] or 1,6-hexandioldimethacrylate [HDMA]) were added (see **Table 1** for the samples composition). The water phase was achieved by dissolving 272 mg of potassium persulfate (KPS), as radical initiator, in the presence or not of PEGMA (see **Table 1**), in nitrogen degassed double distilled water (DDW). The water phase was added drop by drop into the round bottom flask using a dropping funnel. During this procedure, the system was maintained under a continuous stirring (300 rpm) provided by an overhead mechanical stirrer and under a constant nitrogen flow. After the whole internal aqueous phase was added to the oil phase (20 minutes drop by drop), the stirring was increased up to 400 rpm for 1 hour under nitrogen until a white highly viscous biphasic system (high internal phase emulsion) was achieved.

2.3.3 PolyHIPEs preparation; Polymerization step

In order to polymerize the external phase of the HIPEs (to obtain the polyHIPEs), the emulsions were transferred in a PE Syringe connected by a female luer coupler to a second syringe pre-filled with 272 µl of TEMED, **Figure S4**. Using a "syringe-to-syringe" method, HIPEs and TEMED were mixed by an alternate extrusion from one syringe to the other until (12 extrusion processes). The optimal number of extrusions was visually established by using a monomer-soluble dye instead of the radical initiator until color uniformity of the emulsion was reached. The mixed material was then rapidly transferred onto different supports: PTFE (Teflon), glass or PMMA (Plexiglas). The

materials were then modeled as a thin layer, by using a homemade plastic casting blade to control the thickness of the final polymer.

For all materials, the polymerization was carried out for 24 h at room temperature. The monoliths were then washed in order to remove the not crosslinked materials, initiators and water phase. For the washing procedure, the polymerized and crosslinked materials were placed in a 200 ml beaker and different solvents such as DDW (two x 100 ml), MeOH (two x 100 ml), EtOH (two x 100 ml) and, eventually, THF (one step) were used. The materials not subjected to the final washing step in THF were used for the characterizations in terms of swelling and weight loss in water and organic solvents. After the washing step the materials were placed in an oven at 45°C for 24h to remove residual solvents.

2.3.4 Swelling (SW) and weight loss (WL) studies in water and THF

All dried materials, obtained as above described, not subjected to the THF last washing step, were studied in terms of solvent uptake (THF) and extractable matter in both water and organic solvents. Weighed polymeric monoliths (10-15 mg) were selected and their initial weight was registered (Ws). These polyHIPE samples were placed in a beaker containing 20 ml of water or THF for 24 h. Thereafter, the monoliths were rapidly paper blotted on the surface and the weight of the wet polyHIPEs (Wfw) was registered. Finally, the materials were dried in an oven at 40°C (24 h was a suitable time to reach a constant weight) and their final weights were registered as Wfd. For water uptake (swelling) studies, THF only pre-washed samples were used. Swelling and weight loss values of each sample were calculated using the equations below. All determinations were performed in triplicate. Weight loss % and swelling were calculated according to the following equations (the equation terms were defined in the above text):

Equation (1) $WL\%=(Ws-Wfd)/Ws\times100$

Equation (2) $SW=(Wfw-Wfd)/Wfd$

2.3.5 SEM analysis

Scanning electron microscopy analyses were conducted on gold sputtered samples in order to assess the presence of the typical "open-cell" polyHIPE internal structure. SEM images were acquired from different sides, such as upper, lower and internal sides and those from internal side were used for the voids and throats (internal pores) evaluation.

2.3.6 Drug loading of curcumin (CUR)

PolyHIPEs 3.2, 3.5, 3.7, 3.8, 3.11, 3.12, 3.14 and 3.16 were selected to be loaded with curcumin (CUR). For each sample, 200 mg of washed and dried material were weighted. Therefore, a 10 mg/ml CUR solution in THF was prepared and the weighted material was placed into 2 ml of this solution for 24 h. Then, the loaded polyHIPEs were oven-dried in mild conditions at 45°C for 3 h and afterwards in a vacuum desiccator for 12 h to remove the remaining solvent. All these procedures occurred in the dark to avoid the photodegradation of CUR.

2.3.7 Drug release studies

A Phosphate Buffer Saline pH 7.4 (PBS) was prepared with NaCl 8 g, KCl 0.2 g, Na_2HPO_4 1.44 g and KH_2PO_4 0.24 g per 1 L of buffer. For the in vitro release studies, a 3% (w/v) polysorbate 80 solution in PBS pH 7.4 was prepared and used as releasing buffer to assure the sink conditions. For each loaded material, 21 small monoliths (≈ 10 mg) were sampled and each one was placed in 50 mL of release buffer. Therefore, 1 ml of buffer was sampled for 7 established time intervals (every sample was conducted in triplicate) corresponding to 30 min, 1 h, 2 h, 4 h, 6 h, 8 h, 24 h, 48 h, 72 h and 120 h. All procedures were carried out in the dark and at 37 °C. The filtered release solutions, at the established time intervals, were then injected in a HPLC/UV-Vis system. To evaluate the complete CUR dissolution in the release medium (sink conditions), the same amount of curcumin

loaded in the samples was put in 50 mL of release buffer and the solution concentration estimated by HPLC as reported in paragraph 2.2.

2.3.8 Tensile mechanical testing

Dog-bone specimens (type V according to ASTM D638 standard) were prepared for some polyHIPE material compositions. In particular, proper dog-bone dimes were printed in-home with the Objet260 Connex3 3D printer (Stratasys) using a Vero-Stratasys photopolymer resin (see **Figure 1**).

Tensile tests were performed in ambient conditions of temperature and relative humidity using a MTS Insight Testing System device (MTS System Corporation) equipped with a 250 N load-cell, two pneumatic grips, and a video extensometer (model ME-46 Messphysik, Fürstenfeld, Austria). All specimens were loaded at a constant cross-head speed of 1 mm/min until to specimen break.

Strain and stress were computed as $\varepsilon = (l - l_0)/l_0$, and $\sigma = F/A_0$, respectively, with l and l_0 the current and initial gauge lengths, F the applied load, A_0 the initial cross sectional area. Tensile properties were determined from the stress/strain plots according to the ASTM D-638 standard. In particular, the tensile strength was identified as the stress at break point, and the Young modulus was computed as the slope of the initial linear portion of the stress/strain curve. Moreover, the strain at break point was also identified.

2.3.9 Compression mechanical testing

Cylindrical specimens (12 mm of diameter and 4 mm of height, ratio 3:1) were prepared for some polyHIPE material compositions. In particular, cylindrical dimes in photopolymer resin were printed again using the Objet 260 Connex 3D printer (see Figure 1).

For compression tests, the MTS system was equipped with a 10 kN load-cell and two compression plates, whereas the video extensometer was not used due to the specimen shortness. All specimens were compressed at a cross-head speed of 1 mm/min until the crash of the two plates.

Strain and stress were computed as $\varepsilon = (l - l_0)/l_0$, and $\sigma = F/A_0$, respectively, with l and l_0 the current and initial height of the specimen, F the applied load, A_0 the initial cylinder section area.

The compressive properties were determined from the stress/strain plots according to the ASTM D-1621 standard. In particular, after correcting for zero strain, the compressive modulus was computed as the slope of the linear region and the compressive strength as the stress at the yield point or the stress at 10 % strain, if such a deformation occurs before the yield point, or in the absence of such a yield point. Finally, the stress at crush point (i.e., crush strength) was identified.

Figure 1. 3D printed molds in photopolymer resin and corresponding polyHIPE specimens; a) Dog-bone specimen (type V according to ASTM D638 standard) for tensile tests b) cylindrical specimens (12 mm of diameter and 4 mm of height, ratio 3:1) for compression test.

2.3.10 Cell culture

Human fibroblasts were obtained from informed donors subjected to skin biopsy. Skin samples were enzymatically digested (0.125% trypsin and 1% collagenase); obtained fibroblasts were cultured in Dulbecco's Modified Eagle's Medium High Glucose (DMEM-HG), 10% fetal bovine serum (FBS), L-glutamine (1.8 mM), penicillin (100 IU/ml), streptomycin (100 µg/ml) and amphotericin B (2.5 µg/ml). Culture medium was refreshed 2 times per week until cell subconfluence. For this experiment, we considered cells cultured until third culture passage.

2.3.11 Cytotoxicity tests

To evaluate the biocompatibility of scaffolds (sample ID: 3.2, 3.5, 3.7, 3.8, 3.10, 3.11, 3.14, 3.15, 3.16), we considered two types of cytotoxicity assay: extract, namely indirect (the material-conditioned medium was used for cell culture), and direct contact cytotoxicity assays. All the samples were sterilized by autoclaving at 121 °C for 20 min before cell testing.

Human fibroblasts were seeded in 96-well plate (10,000 cells/cm^2). After 24 hours, media were discarded and 100 µl of samples were added for 24 hours of incubation.

For indirect method, suitable to detect the effect of soluble substances released by polymeric supports, we previously incubated the scaffolds (2 mg/ml and 4 mg/ml) in culture medium (DMEM-HG with 10% FBS) for 24 hours at 37°C, 5% CO_2; after this time each extract supernatant sample were incubated with fibroblasts for 24 hours.

For direct contact method, scaffolds were shattered in small pieces (0.5 mm^2) and co-incubated (24 hours, 37°C and 5% CO_2) with fibroblasts at two concentrations: 2 mg/ml and 4 mg/ml.

After cell exposure to extracts and scaffolds, viability was evaluated adding 100 ml of 3-(4,5-dimethylthiazol-2-yl)-2,5-diphenyl-tetrazolium bromide (MTT) solution (0.5 mg/ml) in each well. MTT solution was removed after 3 hours of incubation and obtained formazan crystals were dissolved with 100 ml of DMSO. Optical density (OD) of DMSO solution was measured on a microplate reader (Synergy HT, BioTek, UK) at 570 nm and 670 nm (reference wavelength). Cell viability (%) was calculated as follows: 100x(ODs/ODc), where ODs represents the OD mean value of tested sample and ODc is the OD mean value of untreated cells (control). Each condition was tested in triplicate.

2.3.12 Chick embryo choriallantoic membrane (CAM) assay

Fertilized White Leghorn chicken eggs (20 per group) were incubated at 37° C at constant humidity. On day 3, a square window was opened in the shell, and 2 to 3 mL of albumen were

removed to allow detachment of the developing CAM from the shell. The window was sealed with a glass, and the eggs were returned to the incubator. On day 8, eggs were treated with 1 mm^3 fragments of polyHIPEs samples (sterilized by autoclaving at 121 °C for 20 min) or a gelatin sponge soaked with 50 ng vascular endothelial growth factor (VEGF), used as a positive control was placed on the top of the growing CAM, as previously described.[38] CAMs were examined daily until day 12 and photographed *in ovo* with a stereomicroscope equipped with a camera system (Olympus Italia, Rozzano, Italy). At day 12, the angiogenic response was evaluated by image analysis. Briefly, microscopic images obtained from the stereomicroscope were converted in gray-scale and analyzed using the Aperio Positive Pixel Count algorithm embedded in the ImageScope (Leica Biosystems, Nussloch, Germany). The algorithm input parameters were initially set to obtain the identification of pixels related to the blood vessels as strong positive and to the background as medium and weak positive and tuned to minimize non-specific pixel recognition as strong positive. The algorithm output is composed of the number of strong positive pixels (Nsp), the number of medium positive pixels (Np), the number of weak positive pixels (Nwp). A morphometric value is then defined and calculated by the algorithm as: *Number of strong positive pixels* (%) = *Nsp/Np+Nwp+NspX*100. Statistical significance between the stimulated, normal and inhibited experimental groups was assessed by one-way Anova followed by Tukey multiple comparison post-test. The statistical analysis and graph plotting were performed with the Graph Pad Prism 5.0 statistical package (GraphPad Software, San Diego, CA, USA).

2.3.13 Statistical Analysis

For cytotoxicity tests: results obtained from each cytotoxicity assay (direct and indirect) were processed by a multifactor ANOVA, considering sample formulation and concentration as fixed factors, and the viability % as dependent variables. The differences between groups were analyzed with the posthoc LSD's test for multiple comparisons. Unless differently specified, data are expressed as mean ± standard deviation. The statistical significance was fixed at $p<0.05$.

For chick embryo choriallantoic membrane (CAM) assay: data from different experimental groups were compared by a one-way analysis of variance (ANOVA) with $p < 0.05$ at 99% level of confidence (GraphPad Prism v. 4.00 GraphPad Software, Inc., San Diego, CA). Bonferroni post tests were used for post hoc contrast.

3. Result and discussion

3.1 PolyHIPEs preparation and characterization

Here, we set up the preparation of new materials based on polyacrylate/polyacrylate-PEG produced by the high internal phase emulsion technique to provide materials with a suitable internal structure to be exploited for biomedical applications.

In particular, the new materials are intended to be applied on the skin as wound dressings and/or for the controlled release of hydrophobic active principles. The essentially hydrophobic nature of the polyacrylate network was tailored by using a bifunctional crosslinker instead of a trifunctional one (to soften the network increasing its flexibility) and/or by introducing into the network hydrophilic portions of PEG monoacrylate (to make a more hydrophilic network so increasing the amount of incoming water). With these premises, we stabilized an 80 % v/v water phase into 20 % v/v of oil phase (monomers and surfactant) getting a W/O emulsion by using a low HLB surfactant chemically belonging to PEO-PPO-PEO family [poly(ethylene oxide)-poly(propylene oxide)-poly(ethylene oxide)], see **Table 1** for samples composition. These surfactants, commercially known as, e.g., Symperonic® are biocompatible and miscible with the oil (monomers) phase. A so structured emulsion falls within the category of high internal phase emulsions (HIPEs) which we previously explored to produce materials for different biomedical applications.[28, 35]

In the present study we are substantially modifying the chemical composition of the previously prepared polyHIPEs by using a bifunctional crosslinker to improve the materials flexibility and PEG chains to increase the hydrophilicity of the butyl acrylate-based materials. An example of a bended polyHIPE obtained by using the bifunctional crosslinker HDMA is shown in **Figure 2**. Please note that this sample was swollen in THF before bending, in the same conditions the polyHIPEs obtained by the tri-functional crosslinker broke after approximately 50 ° bending.

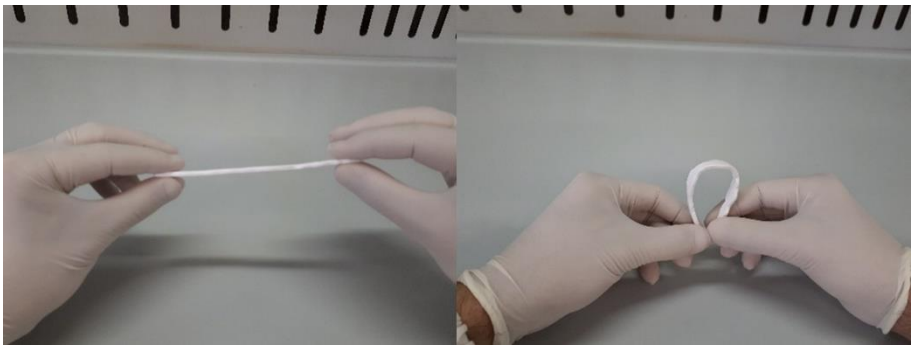

Figure 2. Images showing the flexibility of a representative polyHIPE sample (3.11) obtained with the bifunctional crosslinker HDMA (this sample was preventively swelled in THF).

As first set of experiments, we allowed the HIPEs emulsion to polymerize by casting them on surfaces made from different materials. It was aimed at evaluating the influence of the casting surface on properties such as swelling or weight loss of the polymerized emulsions.

We used glass, plexiglas (polyacrylate) or teflon as the casting bases. The rationale for this choice arises from the different wettability of the emulsion with regard to the casting base other than they are widely used as building materials for e.g. tubes, plates, supports of industrial interest. The contact angle between the emulsion and the surfaces was not evaluated because the emulsion is cream-like so the measurement would not be accurate. Thus, we assumed that the surfaces had comparable roughness. In this way, we thought that the different affinity (in terms of hydrophobic interactions) between the HIPE and the surfaces could lead to unpredictable size pore formation at the interface emulsion/surface depending from their affinity. This would affect the water uptake, by increase or reduction of the polyHIPEs pore size or, for the same reason, the weight loss. In **Table 2** are summarized the main results obtained from this study.

Table 2. Weight loss (WL) and swelling (SW) in water (aq) or tetrahydrofuran (THF) of HIPE samples casted on Teflon (A), Glass (B) or Plexiglas (C). All the samples were tested in triplicate.

Sample	***Surface material***	*WLaq*	*SWaq*	WL_{THF}	SW_{THF}
3.2	A	10.10 ± 0.98	1.69 ± 0,03	6.60 ± 0.28	2.35 ± 0.05
	B	7.29 ± 0.11	2.22 ± 0,14	2.90 ± 0.62	3.93 ± 0.12
	C	6.01 ± 0.56	3.05 ± 0,03	6.01 ± 0.56	4.03 ± 0.69
3.5	A	6.04 ± 0.53	3.10 ± 0.28	4.66 ± 0.36	5.26 ± 0.20
	B	15.72 ± 2.75	2.53 ± 0.25	8.54 ± 1.08	3.91 ± 0.20
	C	1.54 ± 0.30	3.27 ± 0.07	6.25 ± 1.31	5.18 ± 0.34
3.7	A	5.83 ± 1.51	0.98 ± 0.27	8.08 ± 1.57	6.24 ± 0.45
	B	8.37 ± 0,05	3.77 ± 1.55	4,17 ± 1,41	7,35 ± 0,01
	C	2.03 ± 0.85	1.73 ± 0,06	1.48 ± 0.59	7.30 ± 0.12
3.8	A	1.74 ± 0.32	0.57 ± 0.15	1.16 ± 0.19	5.23 ± 0.38
	B	1.33 ± 0.41	1.26 ± 0.40	1.52 ± 0.72	5.71 ± 0.11
	C	2.46 ± 0.15	1.45 ± 0.24	1.68 ± 0.87	4.71 ± 0.33
3.11	A	7.62 ± 0.52	2.73 ± 0.08	5.92 ± 0.09	9.13 ± 0.02
	B	1.61 ± 0.77	4.67 ± 0.01	3.15 ± 0.20	9.04 ± 0.15
	C	2.97 ± 1.87	1.84 ± 0.88	5.09 ± 0.24	8.95 ± 0.56
3.12	A	3.84 ± 0.58	1.20 ± 0.09	2.12 ± 0.88	1.08 ± 0.36
	B	2.77 ± 0.54	0.29 ± 0.03	2.66 ± 0.29	0.38 ± 0.02
	C	1.48 ± 0.01	1.04 ± 0.04	1.00 ± 0.34	1.73 ± 0.24
3.14	A	3.50 ± 0.30	0.39 ± 0.04	0.55 ± 0.15	1.81 ± 0.67
	B	5.22 ± 0.01	0.71 ± 0.04	4.02 ± 0.06	0.80 ± 0.01
	C	6.10 ± 0.79	0.68 ± 0.02	6.07 ± 0.79	0.96 ± 0.08
3.16	A	1.06 ± 0,31	1.4 ± 0.07	2.54 ± 0.35	1.41 ± 0.11
	B	9.06 ± 3,21	1.58 ± 0.11	3.90 ± 1.44	1.01 ± 0.09
	C	6.29 ± 0.79	2.29 ± 0.27	2.79 ± 1.34	1.86 ± 0.14

These results clearly indicate that there are no significant differences in terms of SW or WL between materials obtained by casting and polymerizing them on different surfaces. Only for samples 3.2, 3.8 and 3.16 it looks like the SWaq is increasing in the order Plexiglas > Glass > Teflon but, in general, considering the experimental error, the values can be considered aligned. It

would predict the obtainment of polyHIPEs with similar structure independently from the material used for the emulsion deposition. On the other side, samples 3.12, 3.14 and 3.16 showed low SW values in both water and THF. This behavior could not be simply explained by linking it to the composition, thus further studies were carried out.

We focused our attention on the SEM characterization of the polyHIPEs obtained on Teflon because it is the less chemically reactive support among the tested and gave materials macroscopically well formed.

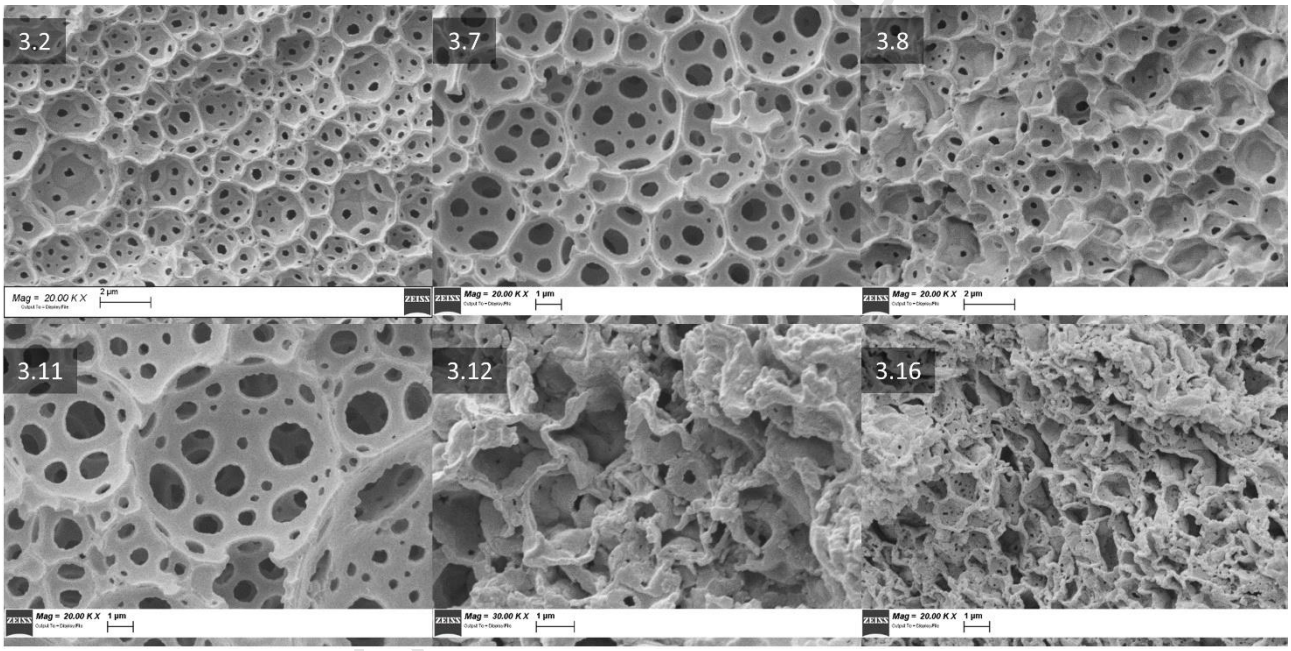

Figure 3. SEM pictures of representative polyHIPEs samples.

From the SEM studies, **Figure 3**, what mostly affects the polyHIPEs internal morphology seems to be the presence or not of PEGMA. In particular sample 3.11 does not contain any PEG and, apart for the void dimensions, also the throats (the holes inside the voids), looks larger and more numerous than in the other samples. The sample 3.16 has the same composition than 3.11 plus PEGMA and shows more collapsed voids with smaller and less numerous throats. The main polyHIPE structure is still maintained. Samples 3.8 and 3.12 have the same monomers composition but different amount in PEGMA, being 0.75 ml in 3.8 and 1.0 ml in 3.12. The higher amount of

PEGMA leads to a more collapsed structure (3.12). Even more evident is the morphologic difference between samples 3.7 and 3.8, the only difference is that 3.8 has PEG while 3.7 not. It is also to be noted that the kind of used crosslinker had a marked effect on the structure, in fact, samples 3.2 and 3.5 (see **Figure S1** for sample 3.5), both containing PEGMA, respectively 0.75 ml and 1.0 ml, but from the trifunctional crosslinker do not show any particular collapse due to the PEG presence even if the throats resulted less numerous and smaller than the counterpart 3.7 without PEG. It could be supposed that the tri-arm crosslinker, such as TMPT, can led to void walls more structured than those formed by using the bifunctional crosslinker HDMA. This would in part compensate the softening action of PEG. To further corroborate this assumption, PEGMA amount was reduced from 1 ml in sample 3.12 to 0.75 ml in sample 3.8 (both crosslinked with HDMA); this led to a more coherent structure similar to the samples 3.2 and 3.5 both crosslinked with TMPT. In conclusion, PEGMA has an evident effect on the polyHIPEs internal structure; the actual amount in the monomers composition allows a precise control of the internal structure.

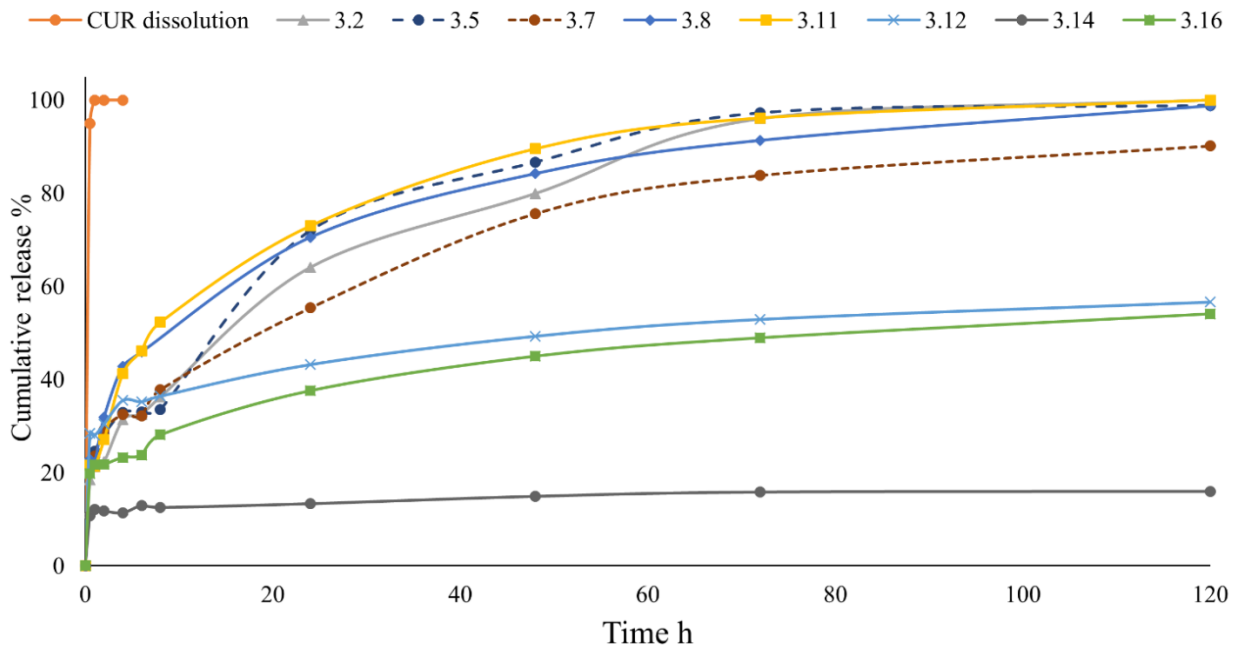

Figure 4. Curcumin release studies from the prepared polyHIPEs, CUR dissolution curve indicates that sink conditions are maintained along the experiment. All the samples had the same drug loading (5 % w/w).

3.3 Drug loading and release

One of the main aims of this study, was to evaluate these materials as drug delivery system for the controlled topical delivery of bioactive molecules. In this context, we selected curcumin as a model active molecule with numerous applications, i.e., in wound healing, cancer treatment and anti-inflammatory activity.[39] Curcumin is a highly hydrophobic drug as several molecules of pharmaceutical interest are, such as steroidal drugs and different antibiotics. Curcumin would benefit from its loading into a partially hydrophobic matrix because it should spread inside the material and would be released when in sink conditions.

To perform the release studies, curcumin has been loaded into the polyHIPEs by solvent (THF) soaking thus, the whole amount of loaded CUR was found into the material and was for all the samples 5 % w/w. THF was chosen because of its affinity toward polyacrylates, its simple removal and low toxicity if compared to other volatile solvents such as chlorinated. The results from drug release studies are shown in **Figure 4**.

From a first view, the release curves are dived in two main groups. The first group formed by most of the samples, namely 3.2, 3.5, 3.7, 3.8 and 3.11, shows a complete (100 %) release in the 100-140 h time range (sample 3.7 reached 100 % release in 140 h). The release rate shows a moderate burst effect at the beginning of the experiment (mostly due to the drug adsorbed on the matrix surface) and an almost constant release rate up to the complete release. The second group of curves formed by samples 3.12, 3.14 and 3.16, does not show a complete release if not a remarkable burst effect in the first hours of the experiment.

Now it is possible to link together the results from swelling, SEM and drug release studies. In particular, samples 3.12, 3.14 and 3.16 are those for which the main behaviors are affected by the presence of PEGMA in the water phase and, even, by its amount. Introducing 1 ml of PEGMA in the composition led to i) low swelling in water and THF ii) a void structure with small or no throats

iii) reduced drug release. As known, both concentration and Mw (that here was maintained constant) of PEG could affect the main behavior of an emulsion. In particular, Papouts and co-workers found that: "For molecular weights below Mw 1000, the polymer serves to modify the water-oil interface with an increase in electrical conductivity. With large chains comparable to the droplet size or larger, the structure of the microemulsion is altered.",[40] in our study we used a PEGMA with a Mw of 2000 Da. It could be supposed that the PEG, above an established concentration, affected the emulsion formation or stability in a way that does not allow the throat formation upon polymerization or reduced it in a significant manner. On the other side, since PEGMA enters in the polyHIPE composition (being a methacrylate), it could change the monomer film microenvironment not allowing the polymeric film contraction (due to PEG softening behaviors) that is necessary for throat formation. In fact, in literature it is reported that the throat formation is due to volume contraction during the conversion of monomers to polymer.[41] These assumptions could well explain the structure we found from SEM which shown closed or almost closed throats within the voids of samples 3.12, 3.14 and 3.16. It would also explain the low swelling and the incomplete drug release.

3.4 Mechanical testing on polyHIPE materials

Tensile and compression tests were performed on specimens of selected polyHIPEs samples in order to investigate the impact of the material composition on mechanical properties. The selection was accomplished to investigate samples with the bifunctional crosslinker or with the tri-arm crosslinker as well as samples with or without PEG. In particular, four material compositions were selected, namely 3.2 (not tested for tensile test) and 3.5 (tri-arm crosslinker/PEG), 3.7 (bifunctional crosslinker) and 3.8 (bifunctional crosslinker/PEG).

Results are summarized in **Table 3** for tensile and compression tests, respectively. Reported moduli, strength and strain data are the corresponding average values among successful tests.

On one hand, our results evidence that in tension the considered polyHIPE samples have the typical behavior of a brittle material, i.e., specimens break without a significant deformation (see **Figure S2**).

In particular, the tensile modulus is lower in samples containing PEG (i.e., 3.5, and 3.8) than in the one without PEG (3.7). Accordingly, we can say that the presence of PEG in the material composition reduces significantly the stiffness of the considered polyHIPEs.

Then, the presence of PEG seems to affect the deformation at break of samples. For example, considering samples with bifunctional crosslinker, the deformation at break is higher for the sample containing PEG (3.8) than for the sample without PEG (3.7) suggesting that the presence of PEG makes the polyHIPEs more deformable. On the contrary, the presence of PEG have no influence on the ultimate tensile strength as shown by the similar values obtained for the samples 3.8 and 3.7.

Finally, the kind of used crosslinker seems to affect the material tensile strength as suggested by the lower value obtained for the sample 3.5 containing tri-arm crosslinker rather than bifunctional crosslinker.

On the other hand, our results evidence, in compression, a softer behavior. The typical stress-strain plot has three regions, namely, initial linear region, plateau region, and bulk compression region (**see Figure S3**).

Again, our results evidence that polyHIPE compressive properties are strongly affected by the presence of PEG. For example, with respect to bifunctional crosslinker samples (i.e., 3.7 and 3.8), the compressive modulus is lower for the sample containing PEG (3.8) than for the sample without PEG (3.7). On the contrary, reducing the amount of PEG in tri-arm crosslinker samples (i.e., 1.00 ml for sample 3.2 *vs* 0.75 ml for sample 3.5) a strong reduction of the compressive modulus is observed (see **Table 3**). Although the presence of PEG has an effect in reducing the compressive modulus at parity of crosslinker, such a difference is not remarkable as for tensile tests.

Table 3. Tensile and compression tests on selected polyHIPEs.

Sample	Tensile modulus [MPa]	Tensile strength [MPa]	Deformation at break [%]	Compressive modulus [MPa]	Compressive strength [MPa]	Crush strength [MPa]
3.2	-	-	-	4.69 ± 0.31	0.40 ± 0.04	58.81 ± 22.41
3.5	15.21 ± 3.81	0.49 ± 0.12	6.08 ± 1.21	2.88 ± 0.18	0.33 ± 0.04	33.12 ± 0.12
3.7	42.04 ± 0.42	0.87 ± 0.13	6.09 ± 1.73	4.82 ± 1.37	0.41 ± 0.10	41.25 ± 16.21
3.8	16.52 ± 4.53	0.91 ± 0.14	19.50 ± 0.91	2.00 ± 0.33	0.24 ± 0.02	56.15 ± 9.53

Finally, it is worth noting that, samples 3.2 and 3.5 partially recover the compressive deformation when compressive plates are moved after the end of the test (see **Figure 5**). On the contrary, the samples 3.7 and 3.8 remain crushed, respectively.

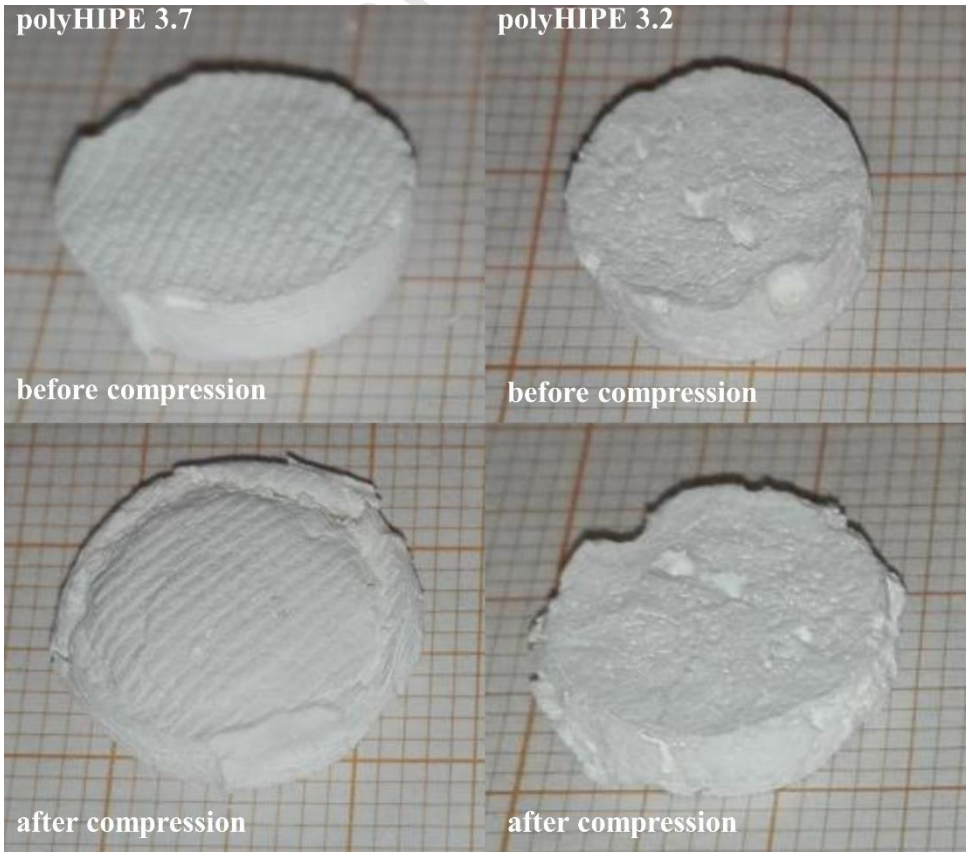

Figure 5. Representative samples 3.7 and 3.2 before (upper pictures) and after (lower picture) the compression test. To be noted the partial recovery of the initial shape by the sample 3.2.

Some works on mechanical characterizations of acrylate based polyHIPEs are available in the literature. For example, Jerenc et al. prepared polyHIPES from monomers such as glycidyl methacrylate (GMA), ethylene glycol dimethacrylate (EGDMA) and 2-ethylhexyl acrylate (EHA). Depending from the relative amount of the monomers, they found different mechanical behaviors either in elongation or compression.[42] In particular, they noted differences in dependence of the EHA amount since by increasing its amount to 5 % w/w the tensile modulus as well as the compressive modulus are reduced accounting this effect to an increased free volume as a consequence of EHA introduction in the composition. In the evaluation of mechanical characteristics of polyHIPEs, even the internal morphology must be taken into account as evidenced by the previous study and by other Authors after filling different polyHIPEs with hydroxyapatite.[43] Both the cited papers link the varied mechanical behaviors of polyHIPEs with their porosity but also with their morphology that, as shown in Figure 3, may change greatly depending on the composition. The dependence of tensile properties on the kind of crosslinker was explored by Caldwell et al. in 2011. They used as crosslinkers the trimethylolpropane triacrylate (TMPTA, the same tri-arm crosslinker we are using in our study) and the dipentaerythritol penta/hexa-acrylate (DPEHA). From the tensile test studies, they found that the polyHIPES obtained with the DPEHA were more stiff than those from TMPTA, so confirming our findings.[44] This is obviously due to the higher crosslinking density gained by using multi-arm crosslinkers that confers higher stiffness at the final material.

Returning to our results, while tensile tests indicated that the polyHIPE samples we tested resulted tendentially brittle materials, the compression data pointed on materials with a certain softness. It looks contradictory but, as mentioned before, the internal structure of the polyHIPE must be accounted as one of the major contributors to the final mechanical properties as well as the chemical

composition. If we think at the polyHIPEs internal structure, we might think at a deflated ball which thickness of the walls can still sustain the main structure. Thus, if the hypothetical ball (the voids in the polyHIPE) is stretched, then it will break upon elongation involving the contiguous voids that will break consequently. When compressed, the walls of the voids will bend in the direction of the applied force and their flexibility will allow some recovery of the original shape.

3.5 Cytocompatibility studies on fibroblasts

Cytotoxicity test on fibroblasts showed a certain variability among the samples, **Figure 6**. The highest viability values were found for samples 3.7, 3.14, 3.15 or 3.16. The last three samples were formed in the presence of PEGMA and by using the bifunctional crosslinker but it is also true that samples 3.14 and 3.16 showed a not complete drug release probably related to their internal structure. No significant differences were found among these samples when the experiment was performed as direct or indirect test at 2 or 4 mg/ml. The two samples crosslinked with the trifunctional reagent, 3.2 and 3.5, showed the lowest cell viability, being the direct method results worse than those from indirect method. For these two samples also the sample concentration played an important role. In particular, sample 3.5 showed a viability lower than 40 % in the direct method at 4 mg/ml. Interestingly, sample 3.10 that is similar in composition to samples 3.15 and 3.16, resulted in a cell viability close to 60 %. While sample 3.11 shown a high cell viability in the indirect method and a still high cell viability for the direct method at 2mg/ml. This sample does not show the PEGMA in its composition. In literature there are not many examples of cell compatibility studies of polyHIPE materials on selected cell lines. One recent paper shows the cell viability of HeLa cells upon incubation with a medium conditioned with the poyHIPE material (indirect method) developed in the study. The Authors stated that "…the polyHIPE leachates had a limited impact on the viability of the cells; each composition remained greater than 70% viable and were therefore considered non-toxic".[37] Their finding perfectly fits with our results obtained for the indirect method. The only difference between the two studies is that we performed the test on

human fibroblasts primary cells (health cells) while the Authors of the referenced paper used immortalized tumor cells.

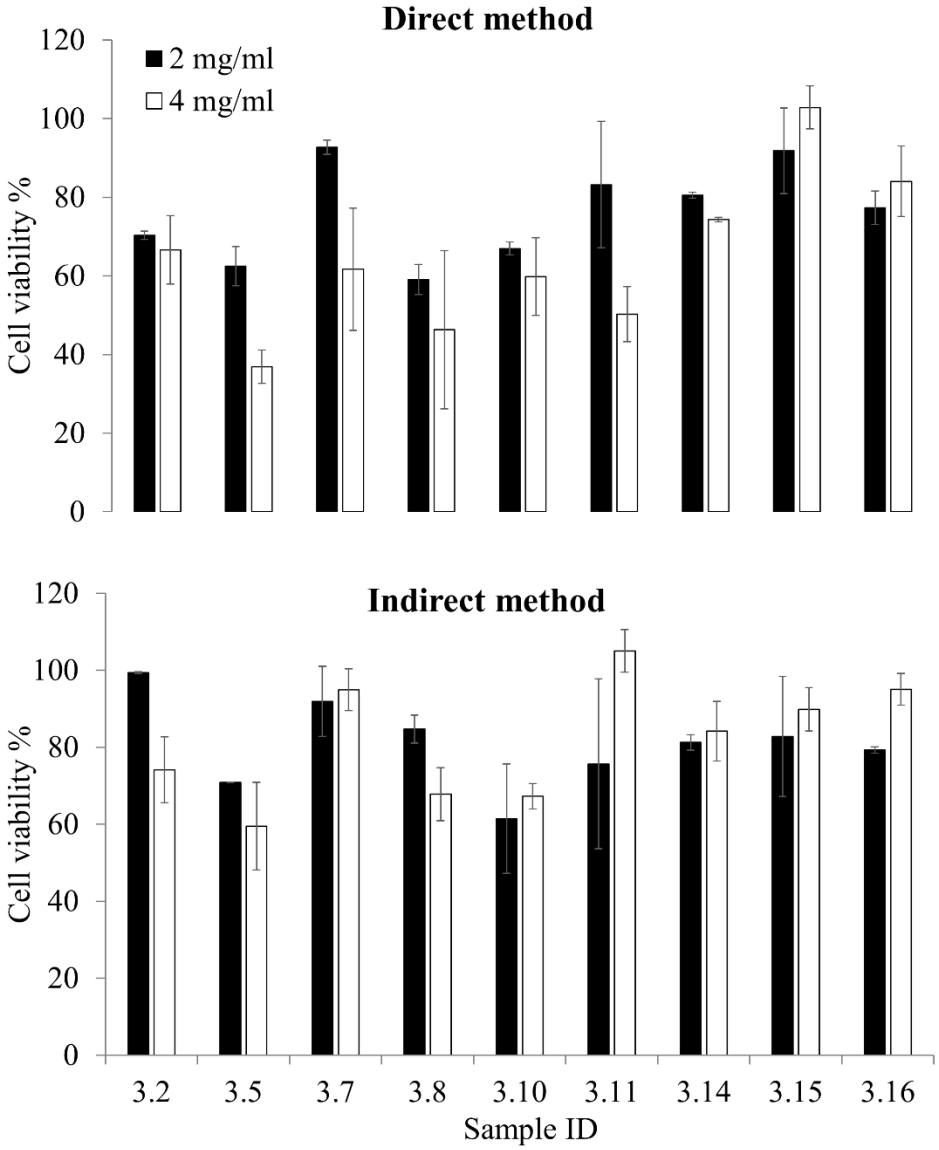

Figure 6. Fibroblast viability for the prepared polyHIPEs by direct contact of the material with the cells (direct method) or by conditioning the culture medium with the materials (indirect test), at two different concentrations 2 or 4 mg/ml.

3.6 Angiogenesis studies by the *in vivo* chick embryo CAM assay

As last characterization, we performed angiogenesis studies by the *in vivo* chick embryo CAM assay. This is a well-established method to evaluate the pro or anti-angiogenic potential of various substances, both in solution or solid form through their direct application on the CAM surface. Since chick embryo at the time of experiment does not possess a yet developed immune system it is not subject to immune response. On the other side, if a well known angiogenic growth factor such as VEGF soaked in a gelatin sponge and applied on the CAM surface, four days after the application, numerous new-formed blood vessels converge toward the sponge, confirming the pro-angiogenic activity of the molecule. On the contrary, when an anti-angiogenic molecule is applied the pre-formed blood vessels around the substance will disappear.

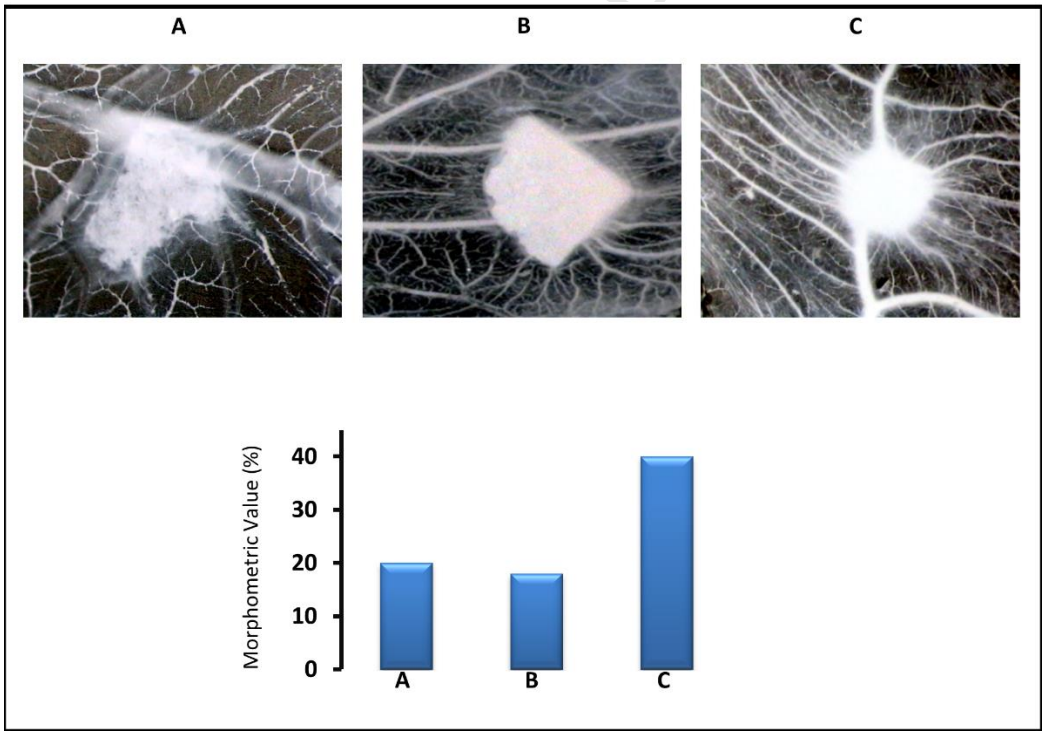

Figure 7. Sample 3.7 (A) or 3.11 (B), and VEGF (positive control) (C) tested by the CAM assay.

From **Figure 7**, it is clear that the applied materials do not have any detectable activity on the CAM vessels, neither pro-angiogenic nor anti-angiogenic. Thus, by an angiogenic point of view these materials could be considered inert, as the number of blood vessels around the samples is

significantly less numerous as compared to the positive control. Considering that the prepared materials are thought for the dermal delivery of hydrophobic drugs it would be a great advantage applying on the skin a material that does not show any kind of angiogenic activity. If a particular angiogenic activity would be required by a specific application, a growth factor or, on the contrary, an anti-angiogenic substance could be added to the final formulation.

As conclusive remarks, based on the collected data, we would assume that PEGMA has an important effect in the emulsion stability and in the monomer film contraction during polymerization. It leads to pore interconnections less numerous and smaller with respect to the samples without PEGMA. Probably, the softening effect of PEG on the main structure also induced some collapsing of the structure itself. The samples 3.7 and 3.11, both obtained from the bifunctional crosslinker, exhibited a controlled release of curcumin up to 5 days and a remarkable cell compatibility.

4. Conclusions

Due to the growing interest on porous materials formed by the polyHIPE technique, this paper focuses on the specific use of these materials for drug delivery applications. At the best of our knowledge, this is among the first examples in literature in which a polyHIPE based biomaterial is used as a DDS. The most engineering aspects are being assessed, such as the obtainment of materials with well-reproducible thickness, shape and actual dimensions. In fact, the prepared samples showed tailorable features in terms of drug release depending on the internal structure.

The possibility to easily sterilize these materials by thermal treatments, the good cytocompatibility and the results obtained from the *in vivo* chick embryo CAM assay showing that the prepared polyHIPEs are neither pro nor anti-angiogenic are fundamental to think at a direct application on wounded tissues after, e.g., the loading of antimicrobial drugs and biological molecules such as growth factors.

Supplementary material

Supplementary material is available from authors.

Conflict of interest statement

We wish to confirm that there are no known conflicts of interest associated with this publication and there has been no significant financial support for this work that could have influenced its outcome.

References

[1] R. Langer, Sci Am 288 (2003) 50-57.
[2] D. Mandracchia, A.P. Piccionello, G. Pitarresi, A. Pace, S. Buscemi, G. Giammona, Macromolecular Bioscience 7 (2007) 836-845.
[3] S.N. Rath, A. Arkudas, C.X. Lam, R. Olkowski, E. Polykandroitis, A. Chroscicka, J.P. Beier, R.E. Horch, D.W. Hutmacher, U. Kneser, J Biomater Appl 27 (2012) 277-289.
[4] T. Garg, A.K. Goyal, Expert Opin Drug Deliv 11 (2014) 767-789.
[5] D. Hutmacher, G.L. Bowlin, J Biomater Sci Polym Ed 19 (2008) 541-542.
[6] G. Pitarresi, G. Tripodo, D. Triolo, C. Fiorica, G. Giammona, Journal of Drug Delivery Science and Technology 19 (2009) 419-423.
[7] C. Dispenza, G. Tripodo, C. LoPresti, G. Spadaro, G. Giammona, Reactive & Functional Polymers 69 (2009) 565-575.
[8] G. Tripodo, T. Chlapanidas, S. Perteghella, B. Vigani, D. Mandracchia, A. Trapani, M. Galuzzi, M.C. Tosca, B. Antonioli, P. Gaetani, M. Marazzi, M.L. Torre, Colloids and Surfaces B-Biointerfaces 125 (2015) 300-308.
[9] S. Abd-Khorsand, S. Saber-Samandari, Int J Biol Macromol 101 (2017) 51-58.
[10] C. Hu, C. Tercero, S. Ikeda, M. Nakajima, H. Tajima, Y. Shen, T. Fukuda, F. Arai, J Biosci Bioeng 116 (2013) 126-131.
[11] Y.S. Nam, J.J. Yoon, T.G. Park, J Biomed Mater Res 53 (2000) 1-7.
[12] R.K. Kankala, Y.S. Zhang, S.B. Wang, C.H. Lee, A.Z. Chen, Adv Healthc Mater 6 (2017).
[13] V. Raeisdasteh Hokmabad, S. Davaran, A. Ramazani, R. Salehi, J Biomater Sci Polym Ed 28 (2017) 1797-1825.
[14] M.S. Silverstein, Progress in Polymer Science 39 (2014) 199-234.
[15] S.D. Kimmins, N.R. Cameron, Advanced Functional Materials 21 (2011) 211-225.
[16] I. Pulko, P. Krajnc, Macromol Rapid Commun 33 (2012) 1731-1746.
[17] D. David, M.S. Silverstein, Journal of Polymer Science Part A: Polymer Chemistry 47 (2009) 5806-5814.
[18] I. Gurevitch, M.S. Silverstein, Macromolecules 44 (2011) 3398-3409.
[19] S. Kovačič, H. Kren, P. Krajnc, S. Koller, C. Slugovc, Macromolecular rapid communications 34 (2013) 581-587.
[20] N.R. Cameron, D.C. Sherrington, L. Albiston, D.P. Gregory, Colloid and Polymer Science 274 (1996) 592-595.
[21] A. Barbetta, N.R. Cameron, Macromolecules 37 (2004) 3188-3201.
[22] V.O. Ikem, A. Menner, T.S. Horozov, A. Bismarck, Advanced Materials 22 (2010) 3588-3592.
[23] X. Yang, L. Tan, L. Xia, C.D. Wood, B. Tan, Macromol Rapid Commun 36 (2015) 1553-1558.
[24] K. Lissant, Emulsions and emulsion technology, CRC Press, 1974.
[25] R. Su, G. Ruan, H. Nie, T. Xie, Y. Zheng, F. Du, J. Li, Journal of Chromatography A 1405 (2015) 23-31.

[26] N.A. Sears, P.S. Dhavalikar, E.M. Cosgriff-Hernandez, Macromolecular rapid communications 37 (2016) 1369-1374.
[27] M. Depardieu, N. Kinadjian, R. Backov, The European Physical Journal Special Topics 224 (2015) 1655-1668.
[28] G. Tripodo, G. Marrubini, M. Corti, G. Brusotti, C. Milanese, M. Sorrenti, L. Catenacci, G. Massolini, E. Calleri, Polymer Chemistry 9 (2018) 87-97.
[29] W. Hu, F. Xie, Y. Li, Z. Wu, K. Tian, M. Wang, L. Pan, L. Li, Langmuir 33 (2017) 13364-13375.
[30] A.J. Wright, M.J. Main, N.J. Cooper, B.A. Blight, S.J. Holder, ACS Appl Mater Interfaces 9 (2017) 31335-31339.
[31] O. Kulygin, M.S. Silverstein, Soft Matter 3 (2007) 1525-1529.
[32] E.M. Christenson, W. Soofi, J.L. Holm, N.R. Cameron, A.G. Mikos, Biomacromolecules 8 (2007) 3806-3814.
[33] Y. Lumelsky, I. Lalush-Michael, S. Levenberg, S. Silverstein Michael, Journal of Polymer Science Part A: Polymer Chemistry 47 (2009) 7043-7053.
[34] S. Dumitriu, Polymeric biomaterials, revised and expanded, Crc Press, 2001.
[35] G. Brusotti, E. Calleri, C. Milanese, L. Catenacci, G. Marrubini, M. Sorrenti, A. Girella, G. Massolini, G. Tripodo, Polymer Chemistry 7 (2016) 7436-7445.
[36] B.C. Streifel, J.G. Lundin, A.M. Sanders, K.A. Gold, T.S. Wilems, S.J. Williams, E. Cosgriff-Hernandez, J.H. Wynne, Macromol Biosci 18 (2018) e1700414.
[37] C.L. McGann, B.C. Streifel, J.G. Lundin, J.H. Wynne, Polymer (United Kingdom) 126 (2017) 408-418.
[38] D. Ribatti, B. Nico, A. Vacca, M. Presta, Nature Protocols 1 (2006) 85-91.
[39] M. Pulido-Moran, J. Moreno-Fernandez, C. Ramirez-Tortosa, M.C. Ramirez-Tortosa, Molecules 21 (2016).
[40] D. Papoutsi, P. Lianos, W. Brown, Langmuir 10 (1994) 3402-3405.
[41] N.R. Cameron, Polymer 46 (2005) 1439-1449.
[42] S. Jerenec, M. Šimić, A. Savnik, A. Podgornik, M. Kolar, M. Turnšek, P. Krajnc, Reactive and Functional Polymers 78 (2014) 32-37.
[43] A. Lee, C.R. Langford, L.M. Rodriguez-Lorenzo, H. Thissen, N.R. Cameron, Biomaterials Science 5 (2017) 2035-2047.
[44] S. Caldwell, D.W. Johnson, M.P. Didsbury, B.A. Murray, J.J. Wu, S.A. Przyborski, N.R. Cameron, Soft Matter 8 (2012) 10344-10351.

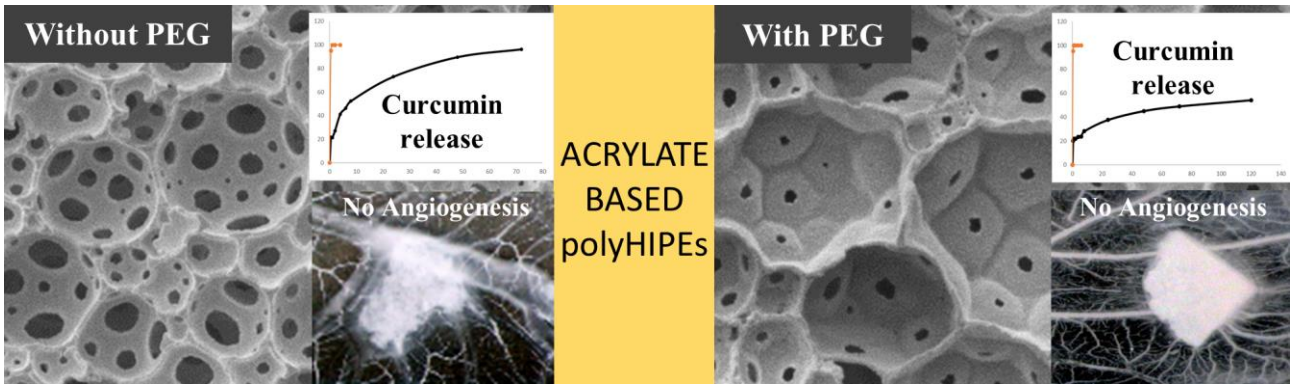

Graphical abstract

Highlights

- Biomaterials from different acrylates and crosslinkers were developed by the high internal phase emulsion technique.
- The different biomaterials obtained were loaded with curcumin and showed differential drug release profiles depending on the composition.
- The polyHIPEs resulted cytocompatible on human fibroblasts.
- The obtained biomaterials resulted neither pro nor anti-angiogenic.